Journal of
Ceramic Science
and Technology

J. Ceram. Sci. Technol., **09** [1] 47-52 (2018)
DOI: 10.4416/JCST2017-00063
available online at: http://www.ceramic-science.com
© 2018 Göller Verlag

Effects of NH_4VO_3 on Properties and Structures of Cordierite Ceramics

W. Ning, Z. Tang, Z. Han, S. Ding, C. Xu, P. Zhang*

Key Laboratory of Automobile Materials of Ministry of Education and College of Materials Science and Engineering, Jilin University, Changchun 130025, China

received July 20, 2017; received in revised form September 25, 2017; accepted November 9, 2017

Abstract

To obtain cordierite ceramics with superior properties, different proportions of NH_4VO_3 were added to a preferred basic ceramic formula, the main raw materials of which included talc, kaolin, calcined kaolin, alumina, aluminum hydroxide and amorphous SiO_2. The cordierite ceramics were manufactured by means of high-temperature sintering. The results show that the coefficient of thermal expansion of the cordierite ceramics is significantly reduced with the addition of 4 % NH_4VO_3; water absorption rate, apparent porosity and flexural strength of the ceramics were increased. The results of FT-IR, XRD and SEM analyses show that V ion entered the lattice of the cordierite crystals and formed V-O bonds and V-O-Si bonds by replacing Mg2+ and Si4+, the strength of the chemical bonds was enhanced during the sintering process. The cell parameters of the cordierite were changed from a = 9.7638 Å, c = 9.3152 Å to a = 9.6851 Å, c = 9.2923 Å. The microcracks in the ceramics disappeared while the pores were increased and uniform. Because of this, the coefficient of thermal expansion is decreased, and the other properties of cordierite ceramics are increased.

Keywords: NH4VO3, cordierite, thermal expansion, structure

I. Introduction

Cordierite ceramics are characterized by a low coefficient of thermal expansion (CTE), high temperature resistance, stable chemical properties, and good dielectric properties. Cordierite ceramics are widely used in many fields, especially as catalyst carrier porcelains and dielectric ceramics. The properties of cordierite ceramics are affected by many factors, including the composition and structure of the raw materials [1–9], the phase composition [10–15] and structure [16–19] of the ceramics. In addition, additives have a great influence on the properties and structure of cordierite ceramics. For example, the glass transition temperature and the crystallization peak temperature are decreased with the addition of 1 wt% B_2O_3 [20]; the formation of α-cordierite was promoted by adding B_2O_3, the growth rate of α-cordierite was increased by adding P_2O_5 [21] to a greater extent than the growth rate of μ-cordierite was increased with the same addition; the conversion rate of the glassy state to the μ-cordierite was accelerated, but the conversion of μ-cordierite to α-cordierite was not affected by the addition of ZnO [22]. The sintering temperature was reduced from 1430 °C to 1050 °C and the CTE was decreased from 1.8×10^{-6} K^{-1} to 1.6×10^{-6} K^{-1} with the addition of 3 % Li_2O-Bi_2O_3 [23]. Sintering, molding and structure of ceramics were affected by the addition of starch [24–26], the CTE of cordierite was reduced to 0.8×10^{-6} K^{-1} with the addition of 10 % starch [27]; the CTE of cordierite was reduced to 0.56×10^{-6} K^{-1} with the addition of a small amount of starch [28].

Gas catalyst carriers are an important application for cordierite ceramics. As these work in alternating hot and cold environments, good thermal shock resistance is essential; hence there is a special requirement for the thermal expansion properties of cordierite ceramics. In order to manufacture cordierite ceramics with superior properties, different proportions of NH_4VO_3 were added to a preferred basic ceramic formula, the main raw materials of which included talc, kaolin, calcined kaolin, alumina, aluminum hydroxide and amorphous SiO_2. The cordierite ceramics were manufactured by means of high-temperature sintering. The effects of NH_4VO_3 on the CTE, water absorption, apparent porosity and flexural strength were investigated; the influence mechanism is discussed based on FTIR, XRD and SEM analyses.

II. Experimental

According to the theoretical composition of cordierite, talc, kaolin, calcined kaolin, alumina, aluminum hydroxide and amorphous SiO_2 were used as raw materials. The diameters of the raw materials ranged from 10 μm to 15 μm. Cordierite ceramics were prepared with different proportions of raw materials. The results concerning the ceramic properties and structures show that the preferred ratio of ceramic raw materials is: talc 37.9 %, kaolin 25.9 %, calcined kaolin 14.7 %, alumina 9.0 %, silica 3.6 %, aluminum hydroxide 8.9 %. Then, 2 %, 4 %, 6 % and 8 %

* Corresponding author: zhangpp@jlu.edu.cn

NH_4VO_3 were added to the basic formulation to manufacture cordierite ceramics. These raw materials were dry-mixed for 5 min to 10 min and molded at 40 MPa pressure. The relationship between temperature and time during the firing process is shown in Fig. 1. The green bodies were heated at the specific rate for each temperature stage and were kept at 1350 °C for 2 h, the cordierite ceramics were then allowed to cool naturally in the furnace. After that, the ceramics were cut into specimens measuring 50 mm × 4 mm × 4 mm. The properties of the specimens were tested and the structures were characterized.

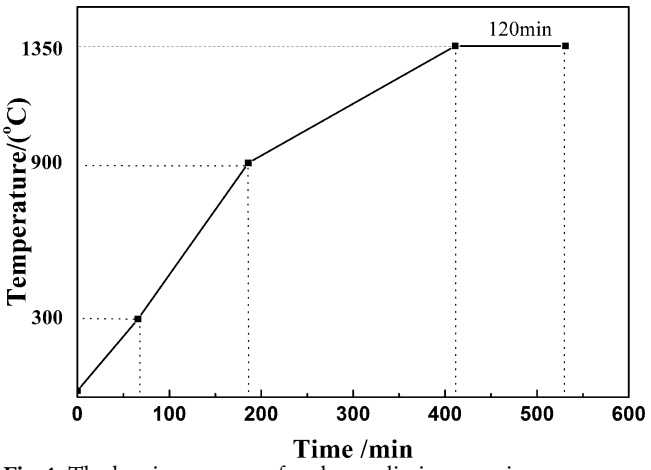

Fig. 1: The heating program for the cordierite ceramics.

III. Results and Discussion

(1) Effects of NH_4VO_3 on the properties of cordierite ceramics

The CTE of the ceramics was measured with a thermal expansion tester (DIL402C, Netzsch). The heating rate was 3 K/min. The temperature range was 25 °C – 850 °C. When the temperature was 850 °C, the final results were the average value of three ceramics. The relationship between the CTE and NH_4VO_3 dosage is shown in Fig. 2.

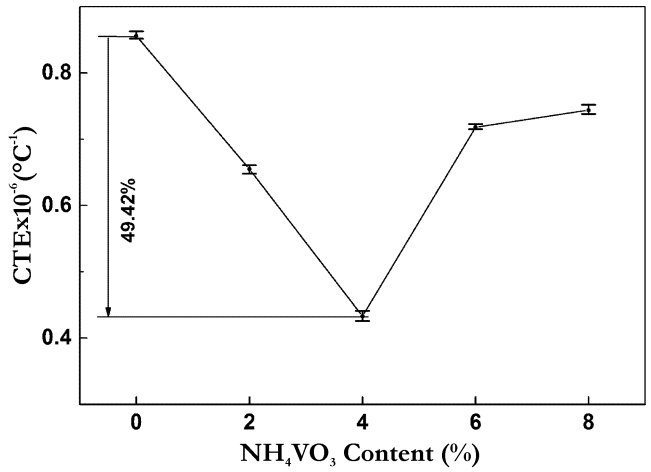

Fig. 2: Effects of the NH_4VO_3 content on the CTE of the cordierite ceramics.

It can be concluded from Fig. 2 that the CTE of the cordierite ceramic was 0.856×10^{-6} K^{-1}. The CTE of ceramics was significantly decreased with the addition of NH_4VO_3. When 4 % NH_4VO_3 was added to the basic formula, the CTE of the cordierite ceramic was 0.433×10^{-6} K^{-1}, that is at the lowest level.

The water absorption rate and apparent porosity of the ceramics were measured with the Archimedes method using distilled water as the medium (TXY-180, China). The final results were the average value of six ceramics. The results are shown in Fig. 3.

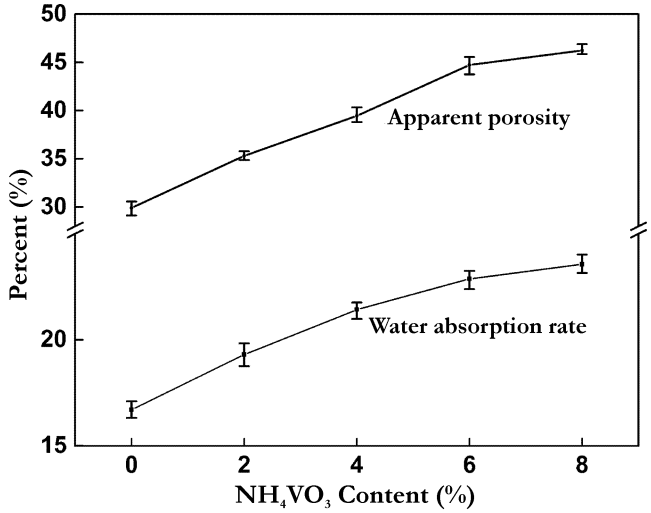

Fig. 3: Effects of the NH_4VO_3 content on the water absorption rate and apparent porosity of the cordierite ceramics.

It can be concluded from Fig. 3 that the water absorption rate and apparent porosity of the cordierite ceramics were significantly increased with the addition of NH_4VO_3. During the sintering process, NH_4VO_3 decomposed and produced gas. NH_4VO_3 played the role of a pore-forming agent, so that the water absorption and apparent porosity of the ceramics were increased.

The flexural strength of the ceramics was tested with a material mechanics tester (MTS-810, America) by using a three-point bending method at a speed of 0.5 mm/min. The final results were the average value of six ceramics. The results are shown in Fig. 4.

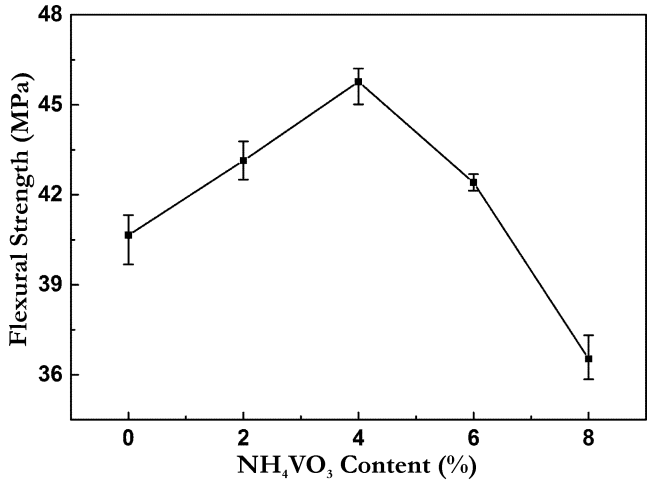

Fig. 4: Effects of the NH_4VO_3 content on the flexural strength.

It can be concluded from Fig. 4 that the flexural strength of the ceramics was increased with the addition of an appropriate content of NH_4VO_3, but the excess NH_4VO_3

led to a decrease in the flexural strength of the ceramics. The maximum flexural strength was 45.77 MPa, when 4 % NH_4VO_3 was added to the basic formula.

(2) Effect of NH_4VO_3 on the structure of cordierite ceramics

(a) *Effect of NH_4VO_3 on the crystal structure of cordierite*

The ceramics were analyzed with an X-ray diffractometer (Rigaku Dmax 2500, Japan). The scanning range was 5 – 60°/2θ, the tube voltage was 50 kV, the tube current was 200 mA, the scanning step was 0.01 mm and the sampling time was 2 s. The XRD pattern of the cordierite ceramic and the vanadium cordierite ceramic is shown in Fig. 5.

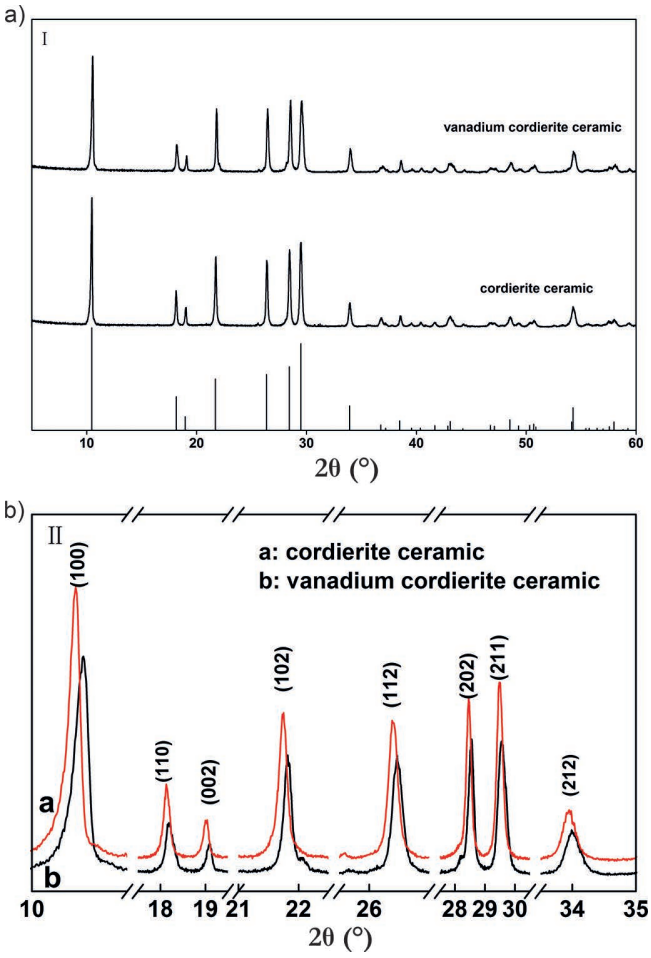

Fig. 5: XRD patterns of the cordierite ceramics.

It can be concluded from Fig. 5 that, after the addition of NH_4VO_3, the main phase of the manufactured ceramics is still cordierite. But the diffraction peaks of the crystal faces showed different degrees of displacement. The cell parameters are calculated based on the d value of the (100) and (002) two crystal faces. The d value of the (100) crystal face ranged from 8.4577 Å to 8.3876 Å and the d value of the (002) crystal face was from 4.6576 Å to 4.6462 Å with the addition of 4 % NH_4VO_3.

So the value of a ranged from 9.7638 Å to 9.6851 Å and the value of c from 9.3152 Å to 9.2923 Å with the addition of 4% NH_4VO_3. In a comparison of the cell parameters, it can be found that the value of a was obviously reduced and the value of c was slightly decreased with the addition of 4 % NH_4VO_3. After the NH_4VO_3 decomposed, V ion entered the cordierite crystal lattice and the lattice was distorted, the a-axis structure became more compact, while the c-axis did not change much.

(b) *Effect of NH_4VO_3 on the chemical structure of cordierite*

The ceramics were tested with a Fourier transform infrared spectrometer (NICOLET760 USA) with a wave number range of 400 – 4000 cm^{-1}. The results are shown in Fig. 6.

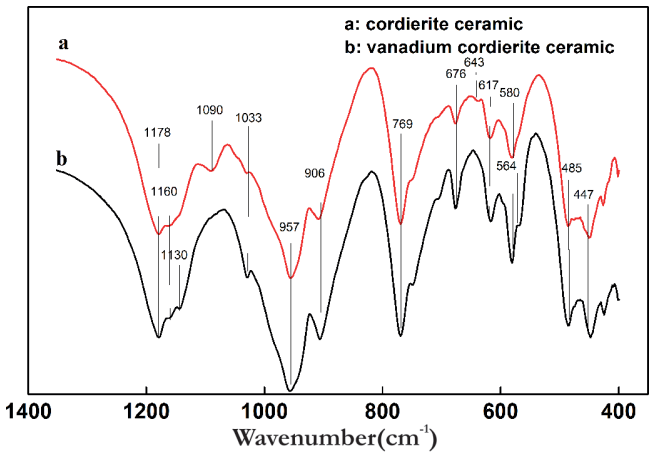

Fig. 6: FI-IR patterns of the cordierite ceramics.

It can be seen from Fig. 6 that the cordierite ceramics' vibration absorption bands are distributed between 1200 cm^{-1} to 400 cm^{-1}. The absorption peaks between 1200 cm^{-1} and 1100 cm^{-1} were caused by Si-O-Si stretching vibration and bending vibration of cordierite silica tetrahedra; the absorption peaks between 1100 cm^{-1} and 900 cm^{-1} were caused by the Al-O stretching vibration and bending vibration of the cordierite aluminum oxide tetrahedra; the absorption peaks between 800 cm^{-1} and 600 cm^{-1} were caused by Mg-O vibration of magnesium oxide octahedra. When compared with the infrared spectra of cordierite ceramics and vanadium cordierite ceramics, the results indicated that the V-O-Si vibration absorption peak of 1130 cm^{-1} and the V-O vibration absorption peak of 564 cm^{-1} appeared; 1090 cm^{-1} Si-O-Si vibration absorption peak and 643 cm^{-1} Mg-O vibration absorption peak were decreased with the addition of the V ion, in the infrared spectrum of cordierite ceramics.

(c) *Effect of NH_4VO_3 on the structure of cordierite ceramics*

The ceramic samples were analyzed with field emission scanning electron microscopy (SEM) (JSM-6700, Japan), the scan voltage was 10 kV. The results are shown in Fig. 7.

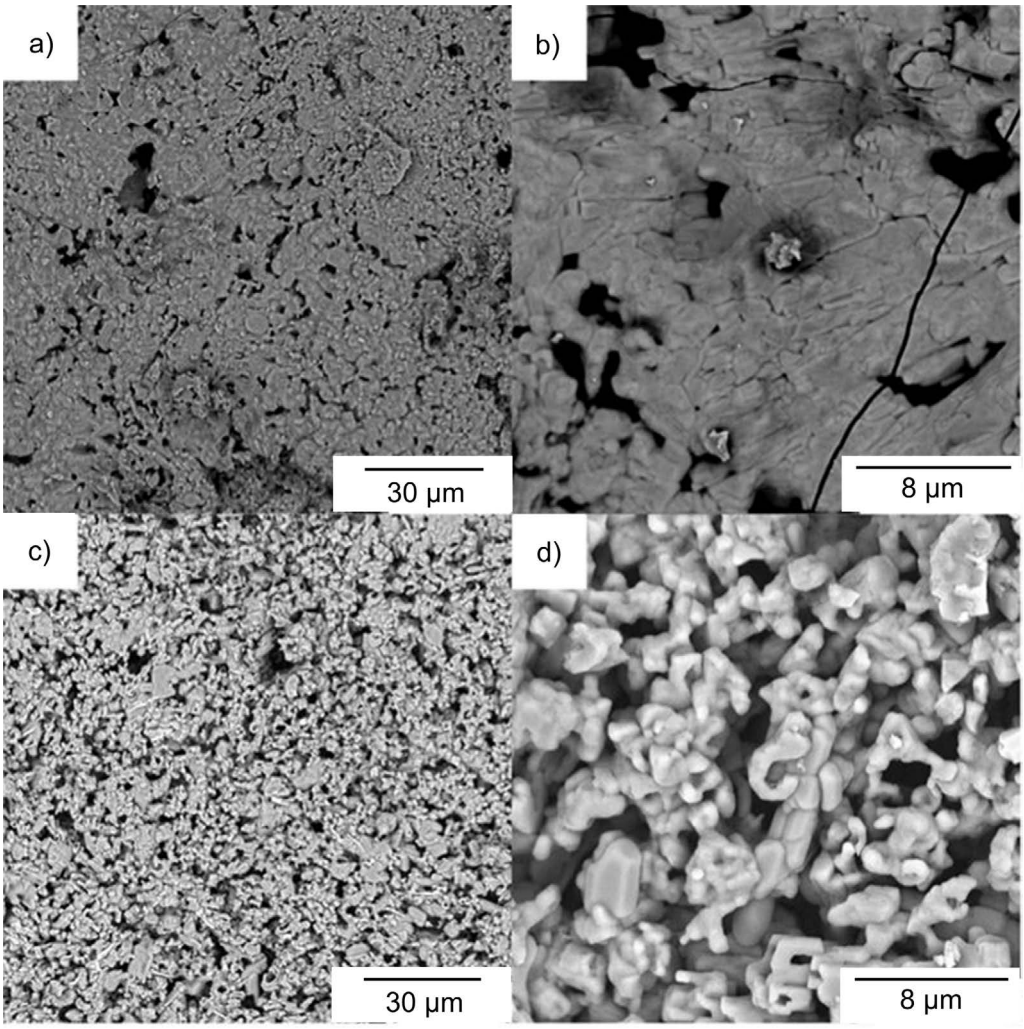

Fig. 7: SEM images of the cordierite ceramics (a, c) and vanadium cordierite ceramics (b, d).

Fig. 7a and b show the scanning electron microscope (SEM) images of the cordierite ceramic in different magnification; and c and d are the SEM images of the vanadium cordierite ceramic at different magnifications. It can be seen from Fig. 7a, the pore diameter of the cordierite ceramic was in the range of 0.63 μm to 17.20 μm; the size of the pores was not uniform and the distribution of pores was not uniform either; the pores accounted for 21.32 % area ratio of the cordierite ceramics. As can be seen from Fig. 7c, the pore diameter of the vanadium cordierite ceramic was in the range of 0.60 μm to 9.72 μm; the pores were uniform in size and the distribution of the pores was relatively uniform; the pores accounted for 30.30 % area ratio of the vanadium cordierite ceramic. When Fig. 7a is compared with Fig. 7c, it can be seen that the size of the ceramic inner pores became smaller, the pores were evenly distributed and the porosity became larger with the addition of 4 % NH_4VO_3. Obvious microcracks in the cordierite ceramics can be observed. The width of cracks extended from 0.10 μm to 0.32 μm and the length of cracks was greater than 20 μm. The crystal grains in the cordierite ceramics were relatively large, the grain size ranging from 2.12 μm × 3.28 μm to 8.56 μm × 4.64 μm, the cordierite grains adhered to each other and were centrally distributed, which further demonstrates that the pore size and distribution were not uniform. It can be seen from Fig. 7d that the vanadium cordierite ceramic grain size was from 1.96 μm × 2.94 μm to 2.96 μm × 7.04 μm and the distribution of vanadium cordierite grains was uniform. The pore diameter of the vanadium cordierite ceramic was in the range of 2.24 μm to 3.44 μm. The pores were evenly distributed and interconnected. There were no obvious microcracks in the vanadium cordierite ceramic. The cordierite ceramic grains were larger than the vanadium cordierite ceramic grains and unevenly distributed, which results from uneven shrinkage of the structure during the crystallization process. That causes the presence of cracks in the ceramics. The vanadium cordierite ceramic grains are relatively small and uniformly distributed, shrinkage of the structure is uniform and does not cause cracks to form during the crystallization process. When the ceramic is exposed to stress, the stress is likely to concentrate in the crack, leading to a reduction in strength. These changes in the microstructure of the ceramics indicate that the porosity, water absorption and flexural strength of ceramics would increase with the addition of NH_4VO_3, which was consistent with the macroscopic performance test results of the ceramics.

(3) Discussion on the impact mechanism

According to the ICSD number of the cordierite PDF card, the α-cordierite crystal structure was obtained by Findit software and Diamond software just as shown in Fig. 8. It can be seen that the hexagonal structures consisted of four Si-O tetrahedra and two AlSi-O tetrahedra. The adjacent two layers were staggered by 30° and arranged along the c-axis in the hexagonal structures. The hexagonal was linked together by Al-O tetrahedra and Mg-O octahedra, in which the Al-O tetrahedra and the Mg-O octahedra were connected by a common edge to achieve stable structures of the cordierite crystals.

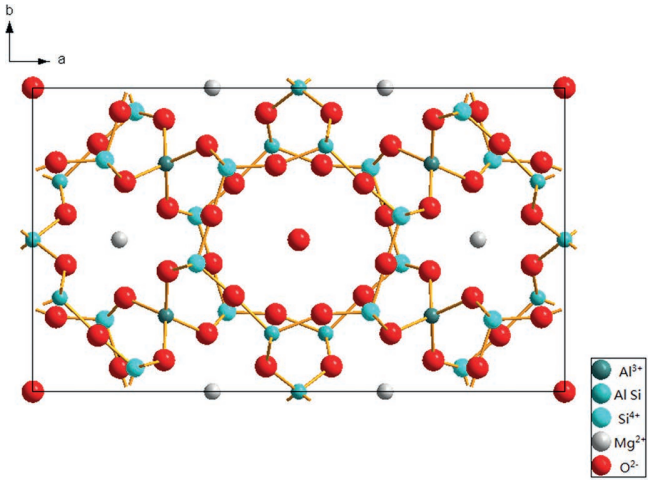

Fig. 8: Crystal structure model of hexagonal cordierite.

The thermal expansion of the crystal is related to the bond length and bond angle of the crystal chemical bond [29]. The thermal deformations of the Mg-O octahedra were the driving force for the thermal expansion of cordierite crystals, because the bond strength between the Mg-O was relatively low, which resulted in expansion along the a axis of the cordierite [30,31].

In a comparison of the infrared spectroscopy of vanadium cordierite and cordierite, the V-O-Si vibration absorption peak at 1130 cm^{-1} and the V-O vibration absorption peak at 564 cm^{-1} appeared, 1090 cm^{-1} Si-O-Si vibration absorption peak and 643 cm^{-1} Mg-O vibration absorption peak decreased with the addition of NH_4VO_3. The results indicated that V ion entered the Si-O tetrahedra and Mg-O octahedra of the cordierite, partially replaced Si^{4+}, Mg^{2+}, and formed V-O-Si bonds and V-O bonds. Since the vanadium ion radius (0.054 nm – 0.064 nm) is smaller than the magnesium ion radius (0.072 nm), the bond length of V-O is smaller than that of Mg-O, the bond strength of V-O is bigger than that of Mg-O and the lattice parameters decreased. So the CTE of the cordierite ceramics was reduced and the mechanical properties were enhanced.

During the sintering of the ceramics, NH_4VO_3 decomposed to produce gas, which led to the formation of pores in the cordierite ceramics. The apparent porosity and water adsorption rate of the ceramics increased and microcracks caused by structural shrinkage during the sintering process were reduced. But excessive addition of NH_4VO_3 led to loose cordierite ceramic crystal structures and the mechanical properties of ceramics were reduced.

IV. Conclusions

1 4 % NH_4VO_3 was added to the base formulation of cordierite ceramic, the coefficient of thermal expansion of the ceramics was effectively reduced and the porosity and mechanical properties of the ceramic were increased.

2 The NH_4VO_3 decomposed during sintering, V ion entered the silicon tetrahedra and magnesia octahedra of cordierite crystals, V ion partially replaced Si^{4+}, Mg^{2+}, and formed V-O-Si bonds and V-O bonds, so that the chemical bond strength of the cordierite crystal was increased while the cell parameters were decreased.

3 The cell parameters of the cordierite crystal were significantly decreased, which was the main reason for the decrease in the coefficient of thermal expansion of the cordierite, while the escape of the NH_3 was the main reason for the increase in the apparent porosity of the ceramic.

4 The introduction of V ions can inhibit the growth of cordierite crystals, resulting in uniform shrinkage of structures, and causing the disappearance of cracks in the ceramics. That increased the strength of the ceramics.

Acknowledgments

The authors gratefully acknowledge the support received from the China Ocean Research Mineral Resources R&D Association (COMRA) Special Foundation (DY135-R2-1-01,DY135-46), and the Province/Jilin University co-construction project-funds for new materials (SXGJSF2017-3).

References

1 Al-Harbi, O.A., Ozgur, C., Khan, M.M.: Fabrication and characterization of single phase cordierite honeycomb monolith with porous wall from natural raw materials as catalyst support, *Ceram. Int.*, **41**, 3526 – 32, (2015).

2 Assebban, M., Tian, Z.-Y., El Kasmi, A., *et al.*: Catalytic complete oxidation of acetylene and propene over clay versus cordierite honeycomb monoliths without and with chemical vapor deposited cobalt oxide, *Chem. Eng. J.*, **262**, 1252 – 59, (2015).

3 Goren, R., Gocmez, H., Ozgur, C.: Synthesis of cordierite powder from talc, diatomite and alumina, *Ceram. Int.*, **32**, 407 – 09, (2006).

4 Kuscer, D., Bantan, I., Hrovat, M., *et al.*: The microstructure, coefficient of thermal expansion and flexural strength of cordierite ceramics prepared from alumina with different particle sizes, *J. Eur. Ceram. Soc.*, **37**, 739 – 46, (2017).

5 Njoya, D., Elimbi, A., Fouejio, D., *et al.*: Effects of two mixtures of kaolin-talc-bauxite and firing temperatures on the characteristics of cordierite-based ceramics, *J. Build. Eng.*, **8**, 99 – 106, (2016).

6 Sembiring, S., Simanjuntak, W., Situmeang, R., *et al.*: Preparation of refractory cordierite using amorphous rice husk silica for thermal insulation purposes, *Ceram. Int.*, **42**, 8431 – 37, (2016).

7 Valaskova, M.: Clays, clay minerals and cordierite ceramics – a review, *Ceram.-Silikaty*, **59**, 331 – 40, (2015).

8 Valášková, M., Martynková, G.S., Smetana, B., *et al.*: Influence of vermiculite on the formation of porous cordierites, *Appl. Clay Sci.*, **46**, 196 – 201, (2009).

[9] Wang, W.B., Shi, Z.M., Wang, X.G., *et al.*: The phase transformation and thermal expansion properties of cordierite ceramics prepared using drift sands to replace pure quartz, *Ceram. Int.*, **42**, 4477 – 85, (2016).

[10] A Hamzawy, E.M., Bin Hussain, M.A.: Sintered gahnite-cordierite glass-ceramic based on raw materials with different fluorine sources, *Bull. Mater. Sci.*, **38**, 1731 – 36, (2015).

[11] Kumar, M.S., Perumal, A.E., Vijayaram, T.R., *et al.*: Processing and characterization of pure cordierite and zirconia-doped cordierite ceramic composite by precipitation technique, *Bull. Mater. Sci.*, **38**, 679 – 88, (2015).

[12] Liu, Y., Luo, F., Su, J.B., *et al.*: Dielectric and microwave absorption properties of Ti_3SiC_2/cordierite composite ceramics oxidized at high temperature, *J. Alloy. Compd.*, **632**, 623 – 28, (2015).

[13] Naga, S.M., Sayed, M., Elmaghraby, H.F., *et al.*: Fabrication and properties of cordierite/anorthite composites, *Ceram. Int.*, **43**, 6024 – 28, (2017).

[14] Xu, X., Zhang, Y., Wu, J., *et al.*: Preparation and performance study of cordierite/mullite composite ceramics for solar thermal energy storage, *Int. J. Appl. Ceram. Tec.*, **14**, 162 – 72, (2017).

[15] Zhang, L.F., Olhero, S., Ferreira, J.M.F.: Thermo-mechanical and high-temperature dielectric properties of cordierite-mullite-alumina ceramics, *Ceram. Int.*, **42**, 16897 – 905, (2016).

[16] Banjuraizah, J., Mohamad, H., Ahmad, Z.A.: Thermal expansion coefficient and dielectric properties of non-stoichiometric cordierite compositions with excess MgO mole ratio synthesized from mainly kaolin and talc by the glass crystallization method, *J. Alloy. Compd.*, **494**, 256 – 60, (2010).

[17] Banjuraizah, J., Mohamad, H., Ahmad, Z.A.: Densification and crystallization of nonstoichiometric cordierite glass with excess MgO synthesized from kaolin and Talc: Densification and crystallization of nonstoichiometric cordierite glass, *J. Am. Ceram. Soc.*, **94**, 687 – 94, (2011).

[18] Ohsato, H., Kim, J.S., Cheon, C.I., *et al.*: Crystallization of indialite/cordierite glass ceramics for millimeter-wave dielectrics, *Ceram. Int.*, **41**, S588 – S93, (2015).

[19] Xu, X.Y., Xu, X.H., Wu, J.F., *et al.*: Fabrication and characterization of cordierite-based glass-ceramic adhesives for bonding solar heat transmission pipelines, *Ceram. Int.*, **43**, 149 – 56, (2017).

[20] Malekzadeh, H., Rezvani, M.: Sol-gel derived cordierite glass-ceramic doped CaO and B_2O_3: Sintering, crystallization and phase transformation characteristics, *J. Sol-Gel Sci. Technol.*, **68**, 128 – 35, (2013).

[21] Wu, J.M., Hwang, S.P.: Effects of (B_2O_3, P_2O_5) additives on microstructural development and phase – transformation kinetics of stoichiometric cordierite glasses, *J. Am. Ceram. Soc.*, **83**, 1259 – 65, (2000).

[22] Clark, S.M.: The kinetic analysis of irreversible consecutive solid state reactions: The effect of zinc on the formation of cordierite, *J. Am. Ceram. Soc.*, **100**, 2525 – 32, (2017).

[23] Ogiwara, T., Noda, Y., Shoji, K., *et al.*: Low temperature sintering of [alpha]-cordierite ceramics with low thermal expansion using Li_2O-Bi_2O_3 as a sintering additive, *J. Ceram. Soc. Jpn.*, **119**, 706, (2011).

[24] Fu, P., Huang, Z., Zhang, F.: A study on preparation of cordierite porous ceramics made from starch Pore-forming agent, *Chem. Eng. Mater. Prop. II*, **549**, 563 – 66, (2012).

[25] Li, Y., Cao, W., Gong, L.L., *et al.*: Effect of starch on sintering behavior for fabricating porous cordierite ceramic, *High Temp. Mater. Proc. (London)*, **35**, 955 – 61, (2016).

[26] Sandoval, M.L., Talou, M.H., Martinez, A.G.T., *et al.*: Starch consolidation casting of cordierite precursor Mixtures: Rheological behavior and green body properties, *J. Am. Ceram. Soc.*, **98**, 3014 – 21, (2015).

[27] Zhu, K., Yang, D., Wu, J., *et al.*: Synthesis of cordierite with low thermal expansion coefficient, *Chinese Ceram. Commun.*, **105 – 106**, 802 – 04, (2010).

[28] Li, Y.L., Liu, J., Hu, H., *et al.*: Effects of potassium and sodium content on properties of cordierite honeycomb ceramic, in chinese, *J. Synth. Cryst.*, **41**, 183 – 187, (2012).

[29] Hochella M.F., Brown G.E.: Structural mechanisms of anomalous thermal expansion of cordierite-beryl and other framework silicates, *J. Am. Ceram. Soc.,* **69**, 13 – 18, (1986).

[30] Ikawa, H., Otagiri, T., Imai, O., *et al.*: Crystal structures and mechanism of thermal expansion of high cordierite and its solid solutions, *J. Am. Ceram. Soc.*, **69**, 492 – 98, (1986).

[31] Predecki, P., Haas, J., Faber, J., *et al.*: Structural aspects of the lattice thermal expansion of hexagonal cordierite, *J. Am. Ceram. Soc.*, **70**, 175 – 82, (1987).